

# Economic Geology

## CONSONORM\_LG: new normative minerals and alteration indexes for low-grade metamorphic rocks --Manuscript Draft--

<b>Manuscript Number:</b>	SEG-D-15-00018
<b>Full Title:</b>	CONSONORM_LG: new normative minerals and alteration indexes for low-grade metamorphic rocks
<b>Article Type:</b>	Regular Paper
<b>Abstract:</b>	<p>The CONSONORM_LG method provides a standardized solution for approximating metamorphic parageneses as well as indexes for estimating chemical and mineralogical changes caused by hydrothermal alteration. CONSONORM_LG is designed for rocks dominated by silicates, Fe-Ti oxides and/or carbonates, and it approximates the main parageneses of greenschist and lower amphibolite-grade metamorphic rocks for three sets of temperature and pressure conditions (2SV350, 2SV450 and 2AMP575 facies of the norm). For each of the facies modelled, the norm calculates the main paragenesis using an ACFMNK tetrahedron, a convenient way of representing a large number of silicate assemblages. In addition to silicate minerals, CONSONORM_LG calculates Fe-Ti oxides and other accessory minerals from minor elements, as well as sulfides from analyzed S or from analyzed metals, and carbonates from analyzed CO<sub>2</sub> or from normative CO<sub>2</sub> estimated from LOI. CONSONORM_LG also calculates several alteration indexes to estimate Fe-Mg (e.g. chloritization), Ca (e.g. propylitic alteration), Na and K acid alterations (e.g. sericitization, phyllic alterations) and Al gain (e.g. argillization). Carbonatation indexes are also calculated using the amount of normative minerals formed by this type of alteration, i.e. carbonates, chlorite and muscovite. The normative calculation is validated using published whole rock analyses and petrographic descriptions. Alteration indexes are validated using several natural samples of alteration halos around base metal and gold deposits.</p>

1  
2  
3  
4 **1 CONSONORM\_LG: new normative minerals and alteration**  
5  
6  
7 **2 indexes for low-grade metamorphic rocks**  
8  
9

10 3 Trépanier, S<sup>a</sup>., Mathieu, L.<sup>b\*</sup>, Daigneault, R<sup>c</sup>.  
11  
12

13 4  
14  
15 <sup>a</sup>Mines Virginia (mining exploration company) – 300 Saint-Paul, suite 200, Québec,  
16  
17  
18 Canada, G1K 7R1  
19

20 7 <sup>b</sup>CONSOREM (Consortium de Recherche en Exploration Minérale - mineral exploration  
21  
22  
23 research consortium), Université du Québec à Chicoutimi (UQAC) – département des  
24  
25  
26 Sciences appliquées, 555 Boul. de l'Université, Chicoutimi, Canada, G7H 2B1.  
27

28 10 <sup>c</sup>Centre d'études sur les Ressources minérales (CERM) - Université du Québec à  
29  
30  
31 Chicoutimi (UQAC) – département des Sciences appliquées, 555 Boul. de l'Université,  
32  
33  
34 Chicoutimi, Canada, G7H 2B1.

35 13 \* Corresponding author: mathiel@tcd.ie, 1-418-545-5011 ext. 2538  
36  
37

38 14  
39

40 15  
41  
42  
43  
44  
45  
46  
47  
48  
49  
50  
51  
52  
53  
54  
55  
56  
57  
58  
59  
60  
61  
62  
63  
64  
65

1  
2  
3  
4  
5  
6  
7  
8  
9  
10  
11  
12  
13  
14  
15  
16  
17  
18  
19  
20  
21  
22  
23  
24  
25  
26  
27  
28  
29  
30  
31  
32  
33  
34  
35  
36  
37  
38  
39  
40  
41  
42  
43  
44  
45  
46  
47  
48  
49  
50  
51  
52  
53  
54  
55  
56  
57  
58  
59  
60  
61  
62  
63  
64  
65

**ABSTRACT**

16  
17 The CONSONORM\_LG method provides a standardized solution for approximating  
18 metamorphic parageneses as well as indexes for estimating chemical and mineralogical  
19 changes caused by hydrothermal alteration. CONSONORM\_LG is designed for rocks  
20 dominated by silicates, Fe-Ti oxides and/or carbonates, and it approximates the main  
21 parageneses of greenschist and lower amphibolite-grade metamorphic rocks for three sets  
22 of temperature and pressure conditions (2SV350, 2SV450 and 2AMP575 facies of the  
23 norm). For each of the facies modelled, the norm calculates the main paragenesis using  
24 an ACFMNK tetrahedron, a convenient way of representing a large number of silicate  
25 assemblages. In addition to silicate minerals, CONSONORM\_LG calculates Fe-Ti oxides  
26 and other accessory minerals from minor elements, as well as sulfides from analyzed S or  
27 from analyzed metals, and carbonates from analyzed CO<sub>2</sub> or from normative CO<sub>2</sub>  
28 estimated from LOI. CONSONORM\_LG also calculates several alteration indexes to  
29 estimate Fe-Mg (e.g. chloritization), Ca (e.g. propylitic alteration), Na and K acid  
30 alterations (e.g. sericitization, phyllic alterations) and Al gain (e.g. argillization).  
31 Carbonatation indexes are also calculated using the amount of normative minerals formed  
32 by this type of alteration, i.e. carbonates, chlorite and muscovite. The normative  
33 calculation is validated using published whole rock analyses and petrographic  
34 descriptions. Alteration indexes are validated using several natural samples of alteration  
35 halos around base metal and gold deposits.

1  
2  
3  
4 39 **1. INTRODUCTION**

5  
6  
7 40 The challenge of exploration geology is to discover and define small-volume  
8  
9 41 concentrations of metals or other economic substances. This search uses vectors as many  
10  
11 42 “footprints” of the mineralizing process. As most deposits are formed by hydrothermal  
12  
13  
14 43 processes, the “footprints” most often sought by exploration geologists are rocks  
15  
16 44 modified by the circulation of hydrothermal fluids. These modifications are either  
17  
18 45 chemical or mineralogical, or both; they are related to metasomatic and alteration  
19  
20  
21 46 processes, respectively (Stanley and Madeisky, 1994) and form what will be designated  
22  
23  
24 47 as altered rocks in this contribution.

25  
26 48 If the recognition of altered rocks is crucial to exploration geology, qualifying and  
27  
28 49 quantifying the alteration is as important in directing the investigations and in identifying  
29  
30  
31 50 the substance most likely to have been concentrated in a given context. The recognition,  
32  
33  
34 51 qualification and quantification of alteration can be approached using various methods  
35  
36 52 briefly summarized here.

37  
38 53 The first is mass balance calculations that use chemical analyses of major elements. In  
39  
40  
41 54 addition, for some methods volatile or trace element analyses might be required. Mass  
42  
43 55 balance methods are based on a mass transfer equation (Gresens, 1967; Stanley and  
44  
45 56 Madeisky, 1994; Leitch and Lentz, 1994) used to compare altered rocks to their un-  
46  
47  
48 57 altered equivalents using ratios of immobile elements to estimate the amount of mass  
49  
50  
51 58 gained and lost by mobile elements (Grant, 1986; Barrett and MacLean, 1994; Stanley  
52  
53 59 and Madeisky, 1994; Trépanier, 2009). The main limit of mass balance methods is the  
54  
55  
56 60 need for a protolith representative of the chemical composition of the fresh precursor of  
57  
58 61 the altered samples. This can be a field sample (Grant, 1986; Barrett and MacLean, 1994)

1  
2  
3  
4 62 or a modelled igneous rock (Trépanier, 2009; Faure et al., 2011; Faure et al., 2014).  
5  
6  
7 63 Another approach is the Pearce Element Ratios – PER method and diagrams (Pearce,  
8  
9 64 1968), which is a method that can be applied to alteration-related mass transfers and that  
10  
11 65 avoids the fresh precursor difficulty (Beswick and Soucie, 1978; Stanley and Madeisky,  
12  
13 66 1994; Nicholls and Gordon, 1994). But the PER technique is difficult to manipulate,  
14  
15  
16 67 especially in an exploration context.

17  
18  
19 68 Alteration can also be approached using alteration indexes often calculated from major  
20  
21 69 element analyses. Most alteration index methods use excesses and deficiencies in major  
22  
23 70 elements to identify the minerals formed or destroyed by an alteration process. For  
24  
25  
26 71 example, the sericite-albite index (Kishida and Kerrich, 1987), the Hashimoto index  
27  
28 72 (Ishikawa et al., 1976) and the alkali index (Saeki and Date, 1980) use  $Al_2O_3$  and alkalis  
29  
30  
31 73 to estimate feldspar destruction and mica formation. Others, such as the chlorite index  
32  
33 74 (Saeki and Date, 1980) and the CCPI-Chlorite-Carbonate-Pyrite index (Large et al.,  
34  
35  
36 75 2001) use FeO and MgO to identify the formation of chlorite or other mafic minerals.  
37  
38 76 The main advantage of alteration indexes is their simplicity; their main disadvantages are  
39  
40  
41 77 their great sensitivity to lithological variations and their poor mineralogical constraints.

42  
43 78 To address this last problem, some indexes are derived from a full normative calculation.  
44  
45  
46 79 For example, the strategy proposed by NORMAT (Piché and Jébrak, 2004) allows for a  
47  
48 80 more precise estimate of the amount of chlorite and white micas for example, likely to be  
49  
50  
51 81 actually present in a rock. The NORMAT method enables the calculation of indexes less  
52  
53 82 sensitive to lithological variations and which do not require the recognition of fresh  
54  
55  
56 83 protoliths.

1  
2  
3  
4  
5  
6  
7  
8  
9  
10  
11  
12  
13  
14  
15  
16  
17  
18  
19  
20  
21  
22  
23  
24  
25  
26  
27  
28  
29  
30  
31  
32  
33  
34  
35  
36  
37  
38  
39  
40  
41  
42  
43  
44  
45  
46  
47  
48  
49  
50  
51  
52  
53  
54  
55  
56  
57  
58  
59  
60  
61  
62  
63  
64  
65

84 Furthermore, and contrary to mass balance calculations, NORMAT requires only major  
85 element analyses and can identify alteration processes involving CO<sub>2</sub> or H<sub>2</sub>O volatiles  
86 based on the analysis of the LOI (Loss On Ignition) (Piché and Jébrak, 2004). NORMAT  
87 is designed for lower greenschist facies rocks and is thus suitable in many shallow  
88 hydrothermal contexts. Also, NORMAT uses a ternary diagram to store its four main  
89 silicate parageneses and uses petrologic rules to calculate hydrothermal and precursor  
90 minerals sequentially. This calculation strategy models hydrothermally altered rocks but  
91 prevents the generalization of the method to other rock types and metamorphic facies;  
92 however, a technique entirely based on thermodynamic equilibrium might be easier to  
93 generalize and may model natural parageneses more accurately.

94 Recognizing the advantages of the normative approach, the authors have built on the  
95 NORMAT method, replacing the ternary diagram by a tetrahedron, adopting a different  
96 calculation sequence and proposing an extension of the norm to mid-grade (this  
97 contribution) and to high-grade metamorphic rocks (Mathieu, 2014). This contribution  
98 extends the method to three low- to mid-grade facies not covered by NORMAT: two  
99 greenschist facies (350<sup>0</sup> C and 450<sup>0</sup> C, 2.5 kbars) and a lower amphibolite facies  
100 (575<sup>0</sup> C, 2 kbars). Among other advantages, the new norm better describes the  
101 mineralogical changes induced by carbonatation. The new method is called the  
102 CONSONORM\_LG norm, with LG standing for “low grade”. It proposes a calculation of  
103 normative minerals and alteration indexes that will be tested on natural examples in the  
104 last section of this contribution.

105  
106 **2. NORMATIVE CALCULATIONS**

1  
2  
3  
4 107 CONSONORM\_LG calculates equilibrium assemblages, i.e. minerals co-existing under  
5  
6 108 given conditions of pressure and temperature, for three sets of conditions: 1) 350<sup>o</sup> C and  
7  
8 109 2.5 kbars (2SV350 facies); 2) 450<sup>o</sup> C and 2.5 kbars (2SV450 facies) and 3) to 575<sup>o</sup> C  
9  
10 and 2 kbars (2AMP575 facies).  
11  
12  
13  
14 111 CONSONORM\_LG norm uses a sequential calculation inspired by the CIPW norm  
15  
16 112 (Cross et al., 1902; 1912), the simultaneous calculation of several minerals proposed by  
17  
18 113 MATNORM (Pruseth, 2009) and the virtual estimation of CO<sub>2</sub> from the LOI, which is an  
19  
20 114 innovation of NORMAT (Piché and Jébrak, 2004). Also, available norms use ternary  
21  
22 115 diagrams (NORMAT; Piché and Jébrak, 2004) or tetrahedrons (MESONORM; Barth,  
23  
24 116 1959) to solve for the main silicate assemblage. Similarly, CONSONORM\_LG uses one  
25  
26 117 tetrahedron per facies. Tetrahedrons are preferred to ternary diagrams because they  
27  
28 118 display a greater number of mineral assemblages which limits the sequential adjustments  
29  
30 119 required to approximate natural parageneses better.  
31  
32  
33  
34  
35  
36  
37

### 3. METAMORPHIC TETRAHEDRONS

38 121  
39  
40 122 Tetrahedrons are the cornerstone of the CONSONORM\_LG calculation and are designed  
41  
42 123 to represent theoretical silicate assemblages for each of the pressure-temperature  
43  
44 124 conditions modelled. The three tetrahedrons used by CONSONORM\_LG consider H<sub>2</sub>O  
45  
46 125 and SiO<sub>2</sub> to be in excess. Their poles correspond to the molar proportions of Al<sub>2</sub>O<sub>3</sub>, CaO,  
47  
48 126 FeO+MgO+MnO and Na<sub>2</sub>O+K<sub>2</sub>O, and are designated as the A, C, FM and NK poles,  
49  
50 127 respectively, of the ACFMNK main tetrahedrons (Fig. 1, 2, 3).  
51  
52  
53 128 Each tetrahedron is an assemblage of four ternary diagrams published by Spear (1993) or  
54  
55 129 modelled by the intermediary of the Theriak-Domino software using the JUN92.BS  
56  
57  
58  
59  
60  
61  
62  
63  
64  
65

1  
2  
3  
4 130 database of thermodynamic data (de Capitani and Petrakakis, 2010). The tetrahedrons  
5  
6  
7 131 were designed by cross-referencing the information provided by the following ternary  
8  
9 132 diagrams:

- 10  
11 133 • Tetrahedron of the 2SV350 facies (Fig. 1): ANK, AKF, AKM, AFM  
12  
13  
14 134 (projected from muscovite) and ACM ternary diagrams from Spear (1993);  
15  
16 135 and a modelled ACK diagram.
- 17  
18  
19 136 • Tetrahedron of the 2SV450 facies (Fig. 2): ACM, ACF, AFM (projected from  
20  
21 137 epidote), ANK, ACM, AKF, AFM, AKM (projected from muscovite) ternary  
22  
23 138 diagrams from Spear (1993); and modelled ACK, ACF and AFM diagrams.
- 24  
25  
26 139 • Tetrahedron of the 2AMP575 facies (Fig. 3): AKM, AKF, AFM (projected  
27  
28 140 from muscovite) and ANK ternary diagrams from Spear (1993); and modelled  
29  
30 141 ACM, ACF, AFM (projected from anorthite) and AKC ternary diagrams.
- 31  
32  
33 142 • The silica deficiency is solved using information provided by ternary diagrams  
34  
35 143 with a pole represented by SiO<sub>2</sub> (diagrams from Spear, 1993).

36  
37  
38 144 The ACFMNK tetrahedrons are designated as the main tetrahedrons, which are made of  
39  
40 145 an assemblage of small tetrahedrons each defined by four minerals (Fig. 1, 2, 3). Also,  
41  
42 146 the paragenesis of FeO- versus MgO-rich rocks and Na<sub>2</sub>O- versus K<sub>2</sub>O-rich rocks can be  
43  
44 147 very different and the full variability of these parageneses cannot be represented on a  
45  
46 148 single tetrahedron. For this reason, the ACFMNK tetrahedrons are designed for MgO-  
47  
48 149 rich and K<sub>2</sub>O-rich rocks and adjustments are made during the norm calculation for rocks  
49  
50  
51 150 rich in FeO and/or Na<sub>2</sub>O (see section 4).

52  
53  
54  
55  
56 151

#### 57 58 152 **4. CALCULATION SEQUENCE**



1  
2  
3  
4 153 CONSONORM\_LG is a Visual Basic code provided as supplementary material. This  
5  
6 154 code prompts the user to choose one of three facies to calculate the norm, i.e. the  
7  
8  
9 155 2SV350, the 2SV450 or the 2AMP575 facies, and to choose between using analyzed or  
10  
11 156 modelled values of CO<sub>2</sub>. The code also uses **measured values of FeO and Fe<sub>2</sub>O<sub>3</sub> only**, and  
12  
13  
14 157 the user is encouraged to **either analyze these values or to estimate them from Fe<sub>2</sub>O<sub>3</sub>T**  
15  
16 158 prior to initiating a CONSONORM\_LG calculation. Discussions on strategies for  
17  
18  
19 159 estimating FeO and Fe<sub>2</sub>O<sub>3</sub> can be found in LeMaître (1976).

20  
21 160 Once the calculation is started, CONSONORM\_LG initiates a succession of operations  
22  
23  
24 161 summarized by Fig. 4. The first set of operations aims to extract and prepare the chemical  
25  
26 162 elements for the norm calculation (see step 1 of Fig. 4) and are conducted as follows:

27  
28  
29 163 1) The calculation starts by extracting the main oxides (SiO<sub>2</sub>, Al<sub>2</sub>O<sub>3</sub>, CaO, MgO,  
30  
31 164 FeO, Fe<sub>2</sub>O<sub>3</sub>, MnO, Na<sub>2</sub>O, K<sub>2</sub>O, TiO<sub>2</sub>, P<sub>2</sub>O<sub>5</sub>), volatiles (H<sub>2</sub>O<sup>+</sup>, H<sub>2</sub>O<sup>-</sup>, S, CO<sub>2</sub>, LOI), some  
32  
33  
34 165 trace elements (Cr, Pb, Zn, Ni, Mo, Cu, As) and the TOTAL from the input file.

35  
36 166 2) The elements are then re-calculated to 100% and converted to moles. Note that  
37  
38  
39 167 if a value for TOTAL is not provided by the user, the norm sums the main oxides,  
40  
41 168 volatiles and trace elements in order to re-calculate each analysis to 100%.

42  
43 169 3) If the user chooses to estimate CO<sub>2</sub> normatively, following the method  
44  
45  
46 170 developed by Piché and Jébrak (2004), the **GOI (Gain on Ignition)** is calculated (equation  
47  
48  
49 171 1). The GOI, i.e. the oxidation of the iron contained in sulfides and carbonates during the  
50  
51 172 heating of a sample, is calculated from the amount of iron contained in the normative  
52  
53 173 carbonates and sulfides. Its value is null at this stage and will be adjusted as these  
54  
55  
56 174 minerals are calculated (equation 1).

1  
2  
3  
4 175 
$$\text{GOI}\% = (\text{sulfide}\% * \text{Fe\_molar\_in\_sulfide} * 1.5 + \text{carbonate}\% * \text{Fe\_molar\_in\_carbonate} * 0.5) * 15.998$$
  
5  
6 176 (equation 1)  
7  
8  
9

10 177

11 178 The normative calculation starts with the sequential calculation of accessory minerals, i.e.  
12  
13  
14 179 sulfides, carbonates and Fe-Ti oxides (see step 2 of Fig. 4):  
15

16 180 1) First, galena, sphalerite, millerite, molybdenite, chalcocopyrite, arsenopyrite,  
17  
18  
19 181 pyrite and anhydrite are calculated until exhaustion of sulfur or the metals, including iron.  
20  
21 182 If sulfur was not analyzed, then pyrite will not be calculated and Pb, Zn, Ni, Mo, Cu and  
22  
23  
24 183 As will be combined with a calculated amount of sulfur until exhaustion of these metals.  
25  
26 184 It is strongly recommended to analyze or estimate the amount of sulfur for rocks  
27  
28  
29 185 containing over 1 wt% iron sulfides, otherwise an incorrect amount of iron will be  
30  
31 186 allocated to silicates and carbonates later in the calculation.  
32

33 187 2) The carbonates are then calculated if  $\text{CO}_2 > 0$ . For the 2SV350 and 2SV450  
34  
35  
36 188 facies, carbonates are calculated using a sequence based on that used in NORMAT (Piché  
37  
38  
39 189 and Jébrak, 2004): 1) calculation of calcite; 2) calculation of magnesite and siderite  
40  
41 190 simultaneously; 3) reaction of these minerals to form dolomite and ankerite. For the  
42  
43  
44 191 2AMP575 facies, carbonates are not calculated at this stage because they are not always  
45  
46 192 stable in the presence of quartz (Spear, 1993).  
47

48 193 3) The Fe-Ti oxides are then calculated sequentially using observations made by  
49  
50  
51 194 Spear (1993) on natural rocks. If  $\text{MgO}/(\text{MgO}+\text{FeO}+\text{Fe}_2\text{O}_3)$  molar  $< 0.45$  (Spear, 1993),  
52  
53  
54 195 ilmenite, then magnetite, titanite, rutile and hematite are calculated successively.  
55  
56 196 Otherwise the calculation sequence is titanite, rutile and hematite, which are calculated  
57  
58 197 until exhaustion of  $\text{Fe}_2\text{O}_3$  or/and  $\text{TiO}_2$ .  
59  
60  
61  
62  
63  
64  
65

1  
2  
3  
4 198 4) The GOI is adjusted according to the normative amount of Fe-bearing oxides  
5  
6 199 and carbonates.

7  
8  
9 200  
10  
11 201 The next series of operations aim at calculating the silicates (see step 3 of Fig. 4). The  
12  
13 202 calculation sequence is the following:

14  
15  
16 203 1) The sample is located in one of the small tetrahedrons of the main ACFMNK  
17  
18 204 tetrahedron using the sample's composition in Al-Ca-K-Na-Fe-Mg. This small  
19  
20 205 tetrahedron is identified using the following steps: a) calculation of the barycentric  
21  
22 206 coordinates of the sample using the main tetrahedron as a reference, followed by a  
23  
24 207 conversion to Cartesian coordinates; b) calculation of the barycentric coordinates of the  
25  
26 208 sample using each small tetrahedron as a reference. The small tetrahedron for which the  
27  
28 209 samples' coordinates are all strictly  $> 0$  is the one that contains the sample.

29  
30  
31 210 2) At this stage, the norm calculates the Mg# (i.e.  $\text{MgO}/(\text{MgO}+\text{FeO})$  molar) and  
32  
33 211 the K# (i.e.  $\text{K}_2\text{O}/(\text{K}_2\text{O}+\text{Na}_2\text{O})$  molar) using the amount of FeO, MgO, Na<sub>2</sub>O and K<sub>2</sub>O  
34  
35 212 remaining after the calculation of accessory minerals.

36  
37  
38 213 3) The four minerals represented by the previously selected small tetrahedron are  
39  
40 214 calculated simultaneously by matrix inversion using a method developed by Pruseth  
41  
42 215 (2009). Then, and for the minerals that represent solid solutions between MgO-FeO and  
43  
44 216 Na<sub>2</sub>O-K<sub>2</sub>O, the molar masses are distributed between each mineral species using the Mg#  
45  
46 217 and K# values.

47  
48  
49 218 4) As the ACFMNK tetrahedrons are designed for MgO-rich rocks, adjustments  
50  
51 219 are here made for FeO-rich rocks. These adjustments enable the formation of chloritoid  
52  
53 220 (facies 2SV450) and garnet, staurolite and cordierite (facies 2AMP575) (Table 1).

1  
2  
3  
4 221 5) The ACFMNK tetrahedrons are designed for K<sub>2</sub>O-rich rocks, and adjustments  
5  
6 222 for Na<sub>2</sub>O-rich rocks are necessary. If white micas and alkali feldspars co-exist, K<sub>2</sub>O is  
7  
8 223 attributed to micas preferentially and Na<sub>2</sub>O is increased in feldspars. Also, paragonite and  
9  
10 224 orthoclase are reacted to form albite and muscovite as these minerals do not co-exist  
11  
12 225 according to ANK ternary diagram (Spear, 1993).  
13

14  
15  
16 226 6) Finally, the amount of silicon used by the normative silicates is calculated. If  
17  
18 227 the silicates' silicon content is less than the amount of SiO<sub>2</sub> available, then quartz is  
19  
20 228 formed; otherwise the silicon deficit is addressed by turning SiO<sub>2</sub>-rich minerals into less  
21  
22 229 SiO<sub>2</sub>-rich phases (Table 2), following the CIPW norm (Cross et al., 1902; 1912).  
23

24  
25  
26 230

27  
28 231 At this stage, the WITHOUTCO<sub>2</sub> alteration indexes are calculated using the proportions  
29  
30 232 of silicates (wt%) calculated in a carbonate-free paragenesis (see section 5) (Fig. 4).  
31  
32 233 These indexes are thus calculated if CO<sub>2</sub> = 0, which is always the case during the first  
33  
34 234 loop of normative mineral calculations. If the user choses to use the amount of analyzed  
35  
36 235 CO<sub>2</sub>, then the normative minerals are destroyed and the calculation of the norm resumes  
37  
38 236 one time to include the amount of analyzed CO<sub>2</sub> and to enable carbonate formation.  
39  
40 237 Otherwise iteration will be initiated (see next paragraph). The WITHOUTCO<sub>2</sub> indexes  
41  
42 238 will no longer be calculated during successive loops (Fig. 4).  
43  
44  
45  
46  
47

48 239

49  
50 240 If the user chooses to estimate CO<sub>2</sub> normatively, following the Piché and Jébrak method  
51  
52 241 (2004), then the iteration is initiated as follows (step 4 of Fig. 4): firstly, the amount of  
53  
54 242 H<sub>2</sub>O consumed by the hydrous normative minerals (H<sub>2</sub>O\_mineral%) is calculated. Then,  
55  
56 243 the following conditions are checked:  
57  
58  
59  
60  
61  
62  
63  
64  
65

1  
2  
3  
4 244 1) If  $LOI\% > (H_2O\_mineral\% + CO_2\_normative\% + S\_analyzed\% + H_2O\`$   
5  
6 245  $\_analyzed\% - GOI\%)$ , then the amount of  $CO_2\_normative\%$  is **increased by 0.1%**, the  
7  
8  
9 246 normative minerals are destroyed and the calculation resumes from the first step, i.e. the  
10  
11 247 extraction of chemical data. The norm calculation will then be resumed as many times as  
12  
13  
14 248 necessary for the values of  $CO_2\_normative\%$ ,  $H_2O\_mineral\%$  and  $GOI\%$  to be properly  
15  
16 249 adjusted to the  $LOI\%$ . Note that a more accurate estimate of  $CO_2\_normative\%$  will be  
17  
18  
19 250 obtained if the  $LOI$  is carefully measured.

20  
21 251 2) If  $LOI\% \leq (H_2O\_mineral\% + CO_2\_normative\% + S\_analyzed\% + H_2O\`$   
22  
23 252  $\_analyzed\% - GOI\%)$ , the iteration ceases.

24  
25  
26 253

27  
28  
29 254 At this stage the calculation of normative minerals is achieved (see step 5 of Fig. 4). The  
30  
31 255 proportions of minerals (wt%) are estimated and re-calculated to 100%. The density of  
32  
33 256 each sample is also estimated using mineral densities from Piché and Jébrak (2004) and  
34  
35  
36 257 from internet compilations (e.g. <http://webmineral.com> by D. Barthelmy, 2014). Finally,  
37  
38 258 the WITHCO2 alteration indexes are calculated (see section 5).

39  
40  
41 259

42  
43 260 CONSONORM\_LG provides the following outputs to its users:

44  
45 261 1) The proportions (wt%) of all the normative minerals calculated during the first  
46  
47  
48 262 loop (i.e. the WITHOUTCO2 minerals) and calculated by the last calculation loop – all  
49  
50  
51 263 other types of minerals.

52  
53 264 2) The values of the WITHCO2 and WITHOUTCO2 alteration indexes.

54  
55 265 3) The estimated density of the sample.  
56  
57  
58  
59  
60  
61  
62  
63  
64  
65

1  
2  
3  
4 266 4) The TOTALoxide (i.e. the sum of original chemical data prior to re-calculating  
5  
6 267 the analysis to 100%) and the TOTALmineral (i.e. sum of normative minerals prior to re-  
7  
8 268 calculation to 100%) parameters are provided to be used as quality control of the norm –  
9  
10 269 confidence should be accorded to the normative calculation only if these parameters are  
11  
12 270 close to 100%.

13  
14  
15  
16 271 5) The ACFK parameter provides the four minerals of the small tetrahedron  
17  
18 272 selected to represent the main paragenesis.

19  
20  
21 273 6) The EXCESSDEFICIT parameter gives specific information on the calculation  
22  
23 274 performed.

24  
25  
26 275 7) The CO<sub>2</sub>\_normative%, GOI% (equation 1) and H<sub>2</sub>O<sup>+</sup>\_normativeMolar  
27  
28 276 (equation 2) values are also given to the user.

29  
30  
31  
32 277 
$$\text{H}_2\text{O}^+_{\text{normativeMolar}} = (\text{LOI}\% + \text{GOI}\% - \text{S}_{\text{analyzed}}\% - \text{H}_2\text{O}^-_{\text{analyzed}}\% - \text{CO}_2_{\text{normative}}\%) / 9.01$$
  
33  
34 278 (equation 2)

35  
36  
37 279

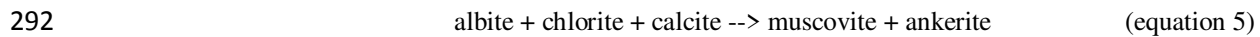
## 38 39 280 **5. ALTERATION INDEXES**

40  
41  
42 281 The alteration indexes compare the proportions of alteration-related minerals and fresh  
43  
44 282 rock-related minerals using ratios (equation 3).

45  
46 283 alteration index = (alteration-related minerals) / (alteration-related minerals + fresh rocks-related minerals)  
47  
48  
49 284 (equation 3)

50  
51 285 Because carbonatation may induce mineralogical changes in a rock without necessarily  
52  
53 286 modifying the absolute concentrations of the main oxides (Kishida and Kerrich, 1987),  
54  
55  
56 287 two main types of indexes are proposed: WITHCO<sub>2</sub> and WITHOUTCO<sub>2</sub>. Indeed,  
57  
58 288 chlorite and muscovite, which are usual markers of FeO, MgO and K<sub>2</sub>O gains, may form

1  
2  
3  
4 289 in FeO-, MgO- or K<sub>2</sub>O-bearing rocks as a result of carbonatation alone (equations 4 and  
5  
6 290 5; after Kishida and Kerrich, 1987).



11  
12 293 The WITHOUTCO<sub>2</sub> indexes are calculated from carbonate-free parageneses, in which  
13  
14  
15 294 the normative muscovite and chlorite can be related to chloritization and sericitization  
16  
17 295 alteration processes with more confidence (Table 3). The WITHOUTCO<sub>2</sub> indexes thus  
18  
19 296 document the Fe-, Mg-, K-, Na- and Ca-types of alterations. On the other hand, the  
20  
21 297 WITHCO<sub>2</sub> indexes use carbonates as well as the normative amounts of **carbonatization**  
22  
23 298 related chlorite and muscovite (Table 4) and are thus dedicated to CO<sub>2</sub>-type of alteration.  
24  
25 299 Note that the 2AMP575 facies, for which carbonates are not calculated, provides only  
26  
27 300 WITHOUTCO<sub>2</sub> indexes.  
28  
29  
30  
31

32  
33 301

## 34 35 302 **6. CASE STUDY**

36  
37 303 In this section, CONSONORM\_LG is used to recalculate the chemical composition of a  
38  
39 304 number of samples. The calculation is performed on altered rocks from the Touquoy and  
40  
41 305 Beaufor gold deposits and from the Hellyer and Montauban VMS deposits, using  
42  
43 306 published analytical data (Prabhu and Webber, 1984; Gemmell and Large, 1992; Bernier  
44  
45 307 and MacLean, 1993; Bierlein and Smith, 2003; Roussy, 2003) (see section 6.3 for a brief  
46  
47 308 description of each deposit). A modern database of fresh magmatic rocks is also used to  
48  
49 309 constrain threshold values for the indexes (section 6.2).  
50  
51  
52  
53

54  
55 310

### 56 57 311 ***6.1. Validating the normative calculation***

1  
2  
3  
4 312 We used published analysis from the Touquoy and Beaufor gold deposits to validate the  
5  
6 313 CONSONORM\_LG calculations, as both the chemistry and petrology of these rocks are  
7  
8  
9 314 published. The petrology data were obtained from quantitative XRD analyses (Touquoy  
10  
11 315 deposit; Bierlein and Smith, 2003) and from observations made in thin sections (Beaufor  
12  
13  
14 316 deposit; Roussy, 2003).

15  
16 317 We performed the CONSONORM\_LG calculations for the 2SV350 facies on bulk  
17  
18 318 samples, using an  $\text{Fe}_2\text{O}_3/\text{Fe}_2\text{O}_3\text{T}$  (wt%) ratio of 0.3 to estimate FeO and  $\text{Fe}_2\text{O}_3$  from  
19  
20 319  $\text{Fe}_2\text{O}_3\text{T}$ , and a normative estimation of  $\text{CO}_2$ . The normative parageneses were then  
21  
22 320 compared to the observed phases (Fig. 5), showing a good correlation between modelled  
23  
24 321 and natural minerals.  
25  
26  
27  
28  
29  
30

## 31 323 *6.2. Lithological dependence of indexes and threshold values*

32  
33 324 The alteration indexes have been calculated for fresh magmatic rocks to establish  
34  
35 325 threshold values. We used the GEOROC database (<http://georoc.mpch-mainz.gwdg.de/>)  
36  
37 326 downloaded in 2014. Rocks that were possibly altered were removed from the database  
38  
39 327 by deleting the analysis with  $\text{LOI} > 3 \text{ wt}\%$  and/or  $\text{CO}_2 > 1 \text{ wt}\%$ . The samples were then  
40  
41 328 classified using their original name in the dataset. These names were validated using the  
42  
43 329 De La Roche et al. (1980) classification – the R1-R2 diagram – and the samples were  
44  
45 330 eventually classified as felsic, intermediate, mafic and ultramafic magmatic rocks (n=  
46  
47 331 1125 samples). Alteration indexes were then calculated for each class, and threshold  
48  
49 332 values corresponding to the maximum value of 80% of each dataset (i.e. 80<sup>th</sup> percentile)  
50  
51 333 were established (Table 5).  
52  
53  
54  
55  
56  
57  
58  
59  
60  
61  
62  
63  
64  
65



1  
2  
3  
4 334 Threshold values are less than 20 for index values that range from 0 to 100, indicating a  
5  
6 335 limited dependency of indexes on the variable composition of unaltered magmatic rocks  
7  
8  
9 336 (Table 5). The ALT\_PHYLLO and ALT\_AND indexes, which are sensitive to the  
10  
11 337 amount of normative aluminosilicates, are particularly low for fresh magmatic rocks.  
12  
13  
14 338 Also, note that threshold values for these indexes, as well as for the indexes that use  
15  
16 339 phyllosilicates, are expected to be higher for fresh sedimentary rocks.  
17  
18  
19 340

### 341 *6.3. Calculating the indexes for hydrothermally altered rocks*

342 **Touquoy gold deposit, Nova Scotia, Canada** – The Touquoy deposit is hosted in  
343 metasilstones (see Hudgins, 1989 for details on the lithology). The alteration halos  
344 surrounding the mineralized veins are characterized by feldspar and chlorite destruction,  
345 as well as carbonates, muscovite and disseminated sulfide formation that reflect gains of  
346 CO<sub>2</sub>, K<sub>2</sub>O, Au, As, S and loss of Na<sub>2</sub>O (Bierlein and Smith, 2003). The veins formed at  
347 250-350<sup>o</sup> C and 1-2 kbars, and were then metamorphosed under mid-greenschist facies  
348 conditions (Reynolds et al., 1987).

349 The samples used here were collected along a drill hole and correspond to unaltered to  
350 intensely altered meta-sedimentary rocks (Bierlein and Smith, 2003). We calculated the  
351 2SV350 facies and indexes using the CONSONORM\_LG method with normative CO<sub>2</sub>  
352 and a Fe<sub>2</sub>O<sub>3</sub>/Fe<sub>2</sub>O<sub>3</sub>T (wt%) ratio of 0.3, or using the analyzed values of CO<sub>2</sub>, FeO and  
353 Fe<sub>2</sub>O<sub>3</sub> whenever possible.

354 The alteration indexes for the 2SV350 facies (Fig. 6A) point to phyllosilicate alteration  
355 (muscovite and ± chlorite) and to carbonatation (carbonates and related chlorite). These  
356 alterations correspond to the K<sub>2</sub>O and CO<sub>2</sub> gains reported by Bierlein and Smith (2003),

1  
2  
3  
4 357 indicating concordance between previously interpreted alterations and  
5  
6 358 CONSONORM\_LG indexes.  
7  
8

9 359

10  
11 360 **Hellyer VMS, Tasmania, Australia** – The Hellyer VMS deposit is hosted by an  
12  
13  
14 361 assemblage of felsic to mafic magmatic and sedimentary rocks (see detailed geology in  
15  
16 362 Jack, 1989; McArthur and Dronseika, 1990; Sharpe, 1991; Gemmelle and Large, 1992;  
17  
18 363 Waters and Wallace, 1992; McArthur, 1996; Solomon and Zaw, 1997). The footwall pipe  
19  
20  
21 364 alteration is zoned with a siliceous core surrounded by chloritic and sericitic zones  
22  
23 365 (Gemmell and Large, 1992; Schardt et al., 2001). The deposit formed at an average  
24  
25 366 temperature of 200-350<sup>o</sup> C and was then weakly deformed and metamorphosed  
26  
27  
28 367 (Gemmell and Large, 1992; Large, 1992).

29  
30  
31 368 The samples used correspond to median values representative of the chemistry of the  
32  
33 369 main alteration zones (Gemmell and Large, 1992), for which the 2SV350 facies and  
34  
35 370 indexes of the CONSONORM\_LG method were calculated using normative CO<sub>2</sub> and a  
36  
37 371 Fe<sub>2</sub>O<sub>3</sub>/Fe<sub>2</sub>O<sub>3</sub>T (wt%) ratio of 0.2.

38  
39  
40 372 The ALT\_CHLO alteration index for the 2SV350 facies (Fig. 6B) is high only for the  
41  
42 373 sample from the chloritic zone. The ALT\_MUSCV points to sericitization in the silicified  
43  
44 374 core and in the muscovite-bearing zones. The ALT\_PHYLLO index confirms that all the  
45  
46 375 zones are rich in phyllosilicates, and the other indexes (i.e. ALT\_CHLO and ALT\_  
47  
48 376 MUSCV) show that the phyllosilicate phase varies from one zone to the next. Also, there  
49  
50  
51 377 is no evidence of **carbonatization** based on the ALT\_MUSCV\_CARBS,  
52  
53 378 ALT\_CHLO\_CC\_TLC and ALT\_CARBS indexes.  
54  
55  
56

57  
58 379  
59  
60  
61  
62  
63  
64  
65

1  
2  
3  
4 380 **Beaufor gold deposit, Abitibi, Québec** – The Beaufor and nearby Perron orebodies are  
5  
6 381 hosted by the dioritic Bourlamaque batholith (see detailed geology by Tremblay, 2001;  
7  
8 382 Tessier, 1990; Belkabir et al., 1993). The mineralized veins are surrounded by zoned  
9  
10 383 alteration halos that grade from carbonate-sericite rocks, albite-rich rocks and mesocratic  
11  
12 384 rocks to unaltered rocks (Roussy, 2003). Most of the Abitibi rocks are at greenschist  
13  
14 385 facies (Goulet, 1978; Jolly, 1978), including the rocks of the Bourlamaque pluton  
15  
16 386 (Campiglio and Darling, 1976).

17  
18 387 The samples used here were published by Roussy (2003). The 2SV350 facies and indexes  
19  
20 388 of CONSONORM\_LG were calculated using normative CO<sub>2</sub> and a Fe<sub>2</sub>O<sub>3</sub>/Fe<sub>2</sub>O<sub>3</sub>T (wt%)  
21  
22 389 ratio of 0.3. The samples were grouped using observations made by Roussy (2003) (Fig.  
23  
24 390 6C). The alteration indexes point toward alterations dominated by carbonatation, which  
25  
26 391 formed carbonates, chlorite and muscovite in the altered rocks. All the rocks, including  
27  
28 392 the rocks of the so called unaltered group, had been carbonatized. The rocks of the albite  
29  
30 393 zone are particularly enriched in carbonates and are poorer in phyllosilicates compared to  
31  
32 394 the other groups of rocks (Fig. 6C).

33  
34 395  
35  
36 396 **Montauban VMS, Québec, Canada** – Montauban is a deformed and metamorphosed  
37  
38 397 Zn-Pb-Cu-Ag-Au deposit of VMS origin (Sangster, 1972; MacLean et al., 1982; Bernier  
39  
40 398 et al., 1987; Morin, 1987) located in the allochthonous monocyclic belt of the Proterozoic  
41  
42 399 Grenville Province (see Rivers (1989) for the main divisions of the Grenville orogeny).  
43  
44 400 The deposit is hosted by biotite gneiss and biotite-muscovite-quartz-feldspar gneiss  
45  
46 401 which likely correspond to meta-felsic magmatic rocks (Prahbu and Webber, 1984). The  
47  
48 402 VMS deposit likely formed in greenschist facies conditions and was then metamorphosed  
49  
50 403 to a maximum of 650<sup>o</sup> C and 4.5 kbars (Bernier, 1992).

1  
2  
3  
4 404 The samples used here were published by Bernier and MacLean (1993) and Prabhu and  
5  
6 405 Webber (1984). The 2AMP575 facies and indexes of CONSONORM\_LG were  
7  
8  
9 406 calculated using normative CO<sub>2</sub> and a Fe<sub>2</sub>O<sub>3</sub>/Fe<sub>2</sub>O<sub>3</sub>T (wt%) ratio of 0.2.

10  
11 407 The rocks of the unaltered group contain some muscovite, cordierite, anthophyllite and  
12  
13  
14 408 biotite based on the alteration indexes (Fig. 6D). The altered rocks have the same  
15  
16 409 paragenesis, but contain excess biotite (in all alteration zones, see ALT\_BIOT index),  
17  
18  
19 410 excess cordierite-anthophyllite (for the cordierite- and sillimanite-bearing groups  
20  
21 411 especially, see ALT\_CRD\_ANT index), excess aluminosilicates (for the nodular  
22  
23 412 sillimanite-bearing rocks only, see ALT\_AND index) and a slight excess in muscovite  
24  
25  
26 413 (for the quartzite unit, see ALT\_MUSC index) (Fig. 6D).

27  
28 414 The hydrothermal alteration associated with the Montauban deposit is mostly marked by  
29  
30  
31 415 cordierite, biotite and anthophyllite. These mafic minerals point toward an Fe-Mg  
32  
33 416 alteration (i.e. chloritization). Note that the potassium in the biotite likely originated from  
34  
35  
36 417 the felsic magmatic precursor and is unlikely to be related to a hydrothermally induced  
37  
38 418 K<sub>2</sub>O gain.

39  
40  
41 419  
42  
43 420  
44

## 45 46 421 **7. CONCLUSIONS**

47  
48 422 CONSONORM\_LG is a new method for the recognition of rocks altered by the  
49  
50  
51 423 circulation of hydrothermal fluids. This normative solution standardizes parageneses,  
52  
53 424 links minerals observed in hand sample to modelled phases and calculates alteration  
54  
55 425 indexes.  
56  
57  
58  
59  
60  
61  
62  
63  
64  
65

1  
2  
3  
4 426 Compared to other methods dedicated to the recognition and quantification of alteration  
5  
6 427 processes, CONSONORM\_LG has the following advantages:

7  
8  
9 428 1) It requires only major element analyses and solutions are available even if only  
10  
11 429 the LOI and  $\text{Fe}_2\text{O}_3\text{T}$  are analyzed (i.e. samples for which  $\text{FeO}$ ,  $\text{Fe}_2\text{O}_3$ ,  $\text{H}_2\text{O}^+$ ,  $\text{H}_2\text{O}^-$  and  
12  
13 430  $\text{CO}_2$  are not available). This is an advantage compared to the mass balance methods that  
14  
15  
16 431 require trace element analyses (Stanley and Madeisky, 1994; Trépanier, 2009; Faure et  
17  
18  
19 432 al., 2011; Faure et al., 2014) and volatile analyses (carbonatation estimates described by  
20  
21 433 Grant (1986)).

22  
23  
24 434 2) CONSONORM\_LG can be applied to any rock type, an advantage compared to  
25  
26 435 the mass balance method of Trépanier (2009) that is designed for magmatic rocks only.

27  
28  
29 436 3) CONSONORM\_LG does not require the identification of a fresh precursor, an  
30  
31 437 advantage compared to most mass balance methods (Grant, 1986; Trépanier, 2009).

32  
33  
34 438 4) CONSONORM\_LG method is particularly high-performing in quantifying  
35  
36 439 carbonatation and discriminating between muscovite and chlorite formed as a result of  
37  
38 440 carbonatation from those formed as a result of K or Fe-Mg alterations (i.e. sericitization  
39  
40  
41 441 and chloritization). Also, its performance for recognizing and quantifying K, Na, Fe-Mg  
42  
43 442 and Ca types of alteration is satisfactory. In addition, the mineralogical concepts used to  
44  
45  
46 443 calculate the CONSONORM\_LG indexes are sounder than those used to calculate major  
47  
48 444 element ratio based indexes.

49  
50  
51 445 5) CONSONORM\_LG has the same advantages as NORMAT (Piché and Jébrak,  
52  
53 446 2004). The tetrahedrons of the CONSONORM\_LG method improve the normative  
54  
55  
56 447 calculation, enabling a more precise characterization of the parageneses and opening the  
57  
58  
59  
60  
61  
62  
63  
64  
65

1  
2  
3  
4 448 door to carrying out normative calculations for high-grade metamorphic rocks  
5  
6 449 (CONSONORM\_HG; Mathieu 2014).  
7  
8  
9 450 CONSONORM\_LG and its alteration indexes represent a new set of tools available to the  
10  
11 451 mining exploration industry or to anyone interested in characterizing hydrothermally  
12  
13 452 induced chemical and mineralogical changes, especially those related to carbonatation  
14  
15  
16 453 processes.  
17  
18  
19 454  
20  
21 455

## 22 23 24 456 **ACKNOWLEDGEMENT**

25  
26 457 The authors warmly thank their colleagues Stéphane Faure, Benoit Lafrance and Silvain  
27  
28 458 Rafini for constructive discussions on this project. They also thank Denys Vermette for  
29  
30  
31 459 contributing his data to the initial project, Michel Jébrak for constructive comments,  
32  
33 460 Geneviève Boudrias for editing the original Consorem report on this work (report written  
34  
35 in French, available online at <http://www.consorem.ca/>, Trépanier, 2012) and Judit  
36 461 Ozoray for correcting this manuscript's spelling. The members of the Consorem group  
37  
38 462 for the years 2011-2012 are also thanked as a group for defining this project and for  
39  
40 463 constructive comments throughout its realization. The CONSONORM\_LG calculation  
41  
42 464 has been available to Consorem members as part of the non-public LithoModeleur  
43  
44 465 software since April 2012, and its users are thanked for constructive comments on the  
45  
46 466 method throughout the years.  
47  
48  
49  
50  
51 467  
52  
53 468  
54  
55 469  
56  
57  
58 470  
59  
60  
61  
62  
63  
64  
65

1  
2  
3  
4  
5  
6  
7  
8  
9  
10  
11  
12  
13  
14  
15  
16  
17  
18  
19  
20  
21  
22  
23  
24  
25  
26  
27  
28  
29  
30  
31  
32  
33  
34  
35  
36  
37  
38  
39  
40  
41  
42  
43  
44  
45  
46  
47  
48  
49  
50  
51  
52  
53  
54  
55  
56  
57  
58  
59  
60  
61  
62  
63  
64  
65

**REFERENCES**

- 471
- 472 Barrett, T.J., and MacLean, W.H., 1994, Chemostratigraphy and hydrothermal alteration  
473 in exploration for VHMS deposits in greenstones and younger volcanic rocks:  
474 Alteration and alteration processes associated with ore-forming systems, Geological  
475 Association of Canada, Short Course Notes, v. 11, p. 433-467.
- 476 Barth, T.F.W., 1959, Principles of classification and norm calculations of metamorphic  
477 rocks: *Journal of geology*, v. 67, p. 135-152.
- 478 Barthelmy, D., 2014, Mineralogy Database website (<http://webmineral.com>).
- 479 Belkabir, A., Robert, F., Vu, L., and Hubert, C., 1993, The influence of dikes on  
480 auriferous shear zone development within granitoid intrusions: the Bourlamaque  
481 pluton, Val-d'Or district, Abitibi greenstone belt: *Canadian Journal of Earth  
482 Sciences* , v. 30(9), p. 1924-1933.
- 483 Bernier, L., 1992, Caractéristiques géologiques, lithogéochimiques et pétrologiques des  
484 gîtes polymétalliques de Montauban et de Dussault./Geological, lithogeochemical  
485 and petrological characteristics of the Mntauban and Dussault polymetallique  
486 deposits: Ministère de l'Énergie et des Ressources du Québec (Geological Survey of  
487 Québec), report DV-92-03, p. 31-34.
- 488 Bernier, L., and MacLean, W.H., 1993, Lithogeochemistry of a metamorphosed VMS  
489 alteration zone at Montauban Grenville Province, Quebec: *Exploration and Mining  
490 Geology*, v. 2, p. 367-386.
- 491 Bernier, L., Pouliot, G., and McLean, W.H., 1987, Geology and metamorphism of the  
492 Montauban gold zone: a metamorphosed polymetallic exhalative deposit, Grenville  
493 Province, Québec: *Economic Geology*, v. 82, p. 2076-2090.

1  
2  
3  
4  
5  
6  
7  
8  
9  
10  
11  
12  
13  
14  
15  
16  
17  
18  
19  
20  
21  
22  
23  
24  
25  
26  
27  
28  
29  
30  
31  
32  
33  
34  
35  
36  
37  
38  
39  
40  
41  
42  
43  
44  
45  
46  
47  
48  
49  
50  
51  
52  
53  
54  
55  
56  
57  
58  
59  
60  
61  
62  
63  
64  
65

494 Beswick, A.E., and Soucie, G., 1978, A correction procedure for metasomatism in an  
495 Archean greenstone belt: *Precambrian Research*, v. 6(2), p. 235-248.

496 Bierlein, F.P., and Smith, P.K., 2003, The Touquoy Zone deposit: an exemple of  
497 "unusual" orogenic gold mineralization in the Meguma terrane, Nova Scotia,  
498 Canada: *Canadian Journal of Earth Sciences*, v. 40, p. 447-466.

499 Campiglio, C., and Darling, R., 1976, The geochemistry of the Archean Bourlamaque  
500 batholith, Abitibi, Québec: *Canadian Journal of Earth Sciences*, v. 13(7), p. 972-986.

501 Cross, W., Iddings, J.P., Pirsson, L.V., and Washington, H.S., 1902, A quantitative  
502 chemicominalogical classification and nomenclature of igneous rocks: *Journal of*  
503 *geology*, v. 10, p. 555-590.

504 Cross, W., Iddings, J.P., Pirsson, L.V., and Washington, H.S., 1912, Modifications of the  
505 "Quantitative System of Classification of Igneous Rocks": *The Journal of Geology*,  
506 v. 20(6), p. 550-561.

507 De Capitani, C., and Petrakakis, K., 2010, The computation of equilibrium assemblage  
508 diagrams with Theriak/Domino software: *American Mineralogist*, v. 95, p. 1006-  
509 1016.

510 De La Roche, H., Leterrier, J., Grandclaude, P., and Marchal, M., 1980, A classification  
511 of volcanic and plutonic rocks using R1-R2-diagram and major-element analyses—  
512 Its relationships with current nomenclature: *Chemical geology*, v. 29(1), p. 183-210.

513 Faure, S., Daigneault, R., Lafrance, B., Rafini, S., and Trépanier, S., 2011, Mineral  
514 exploration problems and real solutions: CONSOREM's contributions to applied  
515 research [ext. abs.]: Québec Exploration meeting, Ministère de l'Énergie et des  
516 Ressources du Québec (Geological Survey of Québec), report DV 2011-04,



1  
2  
3  
4  
5  
6  
7  
8  
9  
10  
11  
12  
13  
14  
15  
16  
17  
18  
19  
20  
21  
22  
23  
24  
25  
26  
27  
28  
29  
30  
31  
32  
33  
34  
35  
36  
37  
38  
39  
40  
41  
42  
43  
44  
45  
46  
47  
48  
49  
50  
51  
52  
53  
54  
55  
56  
57  
58  
59  
60  
61  
62  
63  
64  
65

517 Faure, S., Trépanier, S., and Daigneault, R., 2014, Exploration methods for volcanogenic  
518 massive sulphides in the Abitibi: Contribution of geochemical data processing [ext.  
519 abs.]: Québec Exploration meeting, Ministère de l'Énergie et des Ressources du  
520 Québec (Geological Survey of Québec), report DV 2014-04,  
521 Gemmell, J.B, and Large, R.R., 1992, Stringer system and alteration zones underlying the  
522 Hellyer volcanogenic massive sulfide deposit, Tasmania, Australia: Economic  
523 Geology, v. 83(3), p. 620-649.  
524 GEOROC database, 2014, GEOROC database website ([http://georoc.mpch-](http://georoc.mpch-mainz.gwdg.de/georoc/)  
525 [mainz.gwdg.de/georoc/](http://georoc.mpch-mainz.gwdg.de/georoc/)).  
526 Goulet, N., 1978, Stratigraphy and structural relationships across the Cadillac-Larder  
527 Lake Fault, Rouyn-Beauchastel area, Québec: Ministère de l'Énergie et des  
528 Ressources du Québec (Geological Survey of Québec), report DPV-602, 155 p.  
529 Grant, J.A., 1986, The isocon diagram-a simple solution to Gresen's equation for  
530 metasomatic alteration: Economic Geology, v. 81, p. 1976-1982.  
531 Gresens, R.L., 1967, Composition-volume relationships in metasomatism: Chemical  
532 Geology, v. 2, p. 291-306.  
533 Hudgins, A.B., 1989, Report on geological resource estimates and bulk sample results,  
534 Touquoy Project, Moose River, Halifax County, Nova Scotia: Nova Scotia  
535 Department of Natural Resources, Assessment report,  
536 Ishikawa, Y., Sawaguchi, T., Iwaya, S., and Horiuchi, M., 1976, Delineation of  
537 prospecting targets for Kuroko deposits based on modes of volcanism of underlying  
538 dacite and alteration halos: Mining Geology, v. 26, p. 105-117.

1  
2  
3  
4  
5  
6  
7  
8  
9  
10  
11  
12  
13  
14  
15  
16  
17  
18  
19  
20  
21  
22  
23  
24  
25  
26  
27  
28  
29  
30  
31  
32  
33  
34  
35  
36  
37  
38  
39  
40  
41  
42  
43  
44  
45  
46  
47  
48  
49  
50  
51  
52  
53  
54  
55  
56  
57  
58  
59  
60  
61  
62  
63  
64  
65

539 Jack, D.J., 1989, Hellyer host rock alteration: Unpublished M.Sc. thesis, Hobart,  
540 Tasmanio, University of Tasmania, 182 p.

541 Jolly, W.T., 1978, Metamorphic history of the Archean Abitibi belt: Metamorphism in  
542 the Canadian Shield, Geological Survey of Canada, p. 78-100.

543 Kishida, A., and Kerrich, R.D., 1987, Hydrothermal alteration zoning and gold  
544 concentration at the Kerr-Addison lode gold deposit, Kirkland Lake, Ontario:  
545 Economic Geology, v. 82(3), p. 649-690.

546 Large, R.R., 1992, Australian volcanic-hosted massive sulfide deposits; features, styles,  
547 and genetic models: Economic Geology, v. 87(3), p. 471-510.

548 Large, R.R., Gemmell, J.B., Paulick, H., and Huston, D.L., 2001, The alteration box plot:  
549 A simple approach to understanding the relationship between alteration mineralogy  
550 and lithogeochemistry associated with volcanic-hosted massive sulfide deposits:  
551 Economic Geology, v. 96(5), p. 957-971.

552 Le Maître, R.W., 1976, The chemical variability of some common igneous rock: Journal  
553 of Petrology, v. 7, p. 589-639.

554 Leitch, C.H.B., and Lentz, D.R., 1994, The Gresens approach to mass balance constraints  
555 of alteration systems: methods, pitfalls, examples: Alteration and alteration processes  
556 associated with ore-forming systems: Geological Association of Canada, Short  
557 Course Notes, v. 11, p. 161-192.

558 MacLean, W. H., St. Seymour, K., and Prabhu, M. K., 1982, Sr, Y, Zr, Nb, Ti, and REE  
559 in Grenville amphibolites at Montauban-les-Mines, Québec: Journal of Petrology, v.  
560 19(4), p. 633-644.

- 1  
2  
3  
4 561 Mathieu, L., 2014, Caractéristiques minéralogiques et chimiques des altérations dans les  
5  
6 562 roches de haut grade métamorphique - phase I./ Mineralogical and chemical  
7  
8 563 characteristics of alterations in high grade metamorphic rocks: Consorem report 2013-  
9  
10 564 04 (report in french, available at: [http://www.consorem.ca/rapports\\_publics.html](http://www.consorem.ca/rapports_publics.html)).  
11  
12  
13  
14 565 McArthur, G.J., 1996, Textural evolution of the Hellyer massive sulphide deposit:  
15  
16 566 Unpublished Ph.D. thesis, Hobart, Tasmania, University of Tasmania, 272 p.  
17  
18  
19 567 McArthur, G.J., and Dronseika, E.V., 1990, Que River and Hellyer zinc-lead-silver  
20  
21 568 deposits: Geology of the mineral deposits of Australia and Papua New Guinea,  
22  
23 569 Melbourne, Australian Institute of Mining and Metallurgy, v. 2, p. 1257-1266.  
24  
25  
26 570 Morin, G., 1987, Gîtologie de la région de Montauban./ Gitology of the Montauban  
27  
28 571 region: Unpublished M.Sc. thesis, Montréal, Québec, Université du Québec à  
29  
30 572 Montréal, 59 p.  
31  
32  
33 573 Nicholls, J., and Gordon, T.M., 1994, Procedures for the calculation of axial ratios on  
34  
35 574 Pearce element-ratio diagrams: The Canadian Mineralogist, v. 32(4), p. 969-977.  
36  
37  
38 575 Pearce, T.H., 1968, A contribution to the theory of variation diagrams: Contributions to  
39  
40 576 Mineralogy and Petrology, v. 19(2), p. 142-157.  
41  
42  
43 577 Piché, M., and Jébrak, M., 2004, Normative minerals and alteration indices developed for  
44  
45 578 mineral exploration: Journal of Geochemical Exploration, v. 82, p. 59-77.  
46  
47  
48 579 Prabhu, M.K., and Webber, G.R., 1984, Origin of quartzofeldspathic gneisses at  
49  
50 580 Montauban-les-Mines, Québec: Canadian Journal of Earth Sciences, v. 21(3), p. 336-  
51  
52 581 345.  
53  
54  
55 582 Pruseth, **K.**, 2009, Calculation of the CIPW norm: new formulas: Journal of Earth  
56  
57 583 Science Systems, v. 118(1), p. 101-113.  
58  
59  
60  
61  
62  
63  
64  
65

1  
2  
3  
4  
5  
6  
7  
8  
9  
10  
11  
12  
13  
14  
15  
16  
17  
18  
19  
20  
21  
22  
23  
24  
25  
26  
27  
28  
29  
30  
31  
32  
33  
34  
35  
36  
37  
38  
39  
40  
41  
42  
43  
44  
45  
46  
47  
48  
49  
50  
51  
52  
53  
54  
55  
56  
57  
58  
59  
60  
61  
62  
63  
64  
65

584 Reynolds, P.H., Elias, P., Muecke, G.K., and Grist, A.M., 1987, Thermal history of the  
585 southwestern Meguma zone, Nova Scotia, from an <sup>40</sup>Ar/<sup>39</sup>Ar and fission track  
586 dating study of intrusive rocks: Canadian Journal of Earth Sciences , v. 24(10), p.  
587 1952-1965.

588 Rivers, T., Martignole, J., Gower, C.F., and Davidson, A., 1989, New tectonic divisions  
589 of the Grenville Province, southeast Canadian Shield: Tectonics, v. 8(1), p. 63-84.

590 Roussy, J., 2003, Relations entre la distribution de l'or, la structure, la composition des  
591 veines et de l'altération hydrothermale à la mine Beaufor, Val d'Or, Québec./  
592 Relationships between gold distribution, structure, veines composition and  
593 hydrothermal alteration at the Beaufor mine, Val d'Or, Québec: Unpublished M.Sc.  
594 thesis, Montréal, Québec, Laval university, 311 p.

595 Saeki, Y., and Date, J., 1980, Computer application to the alteration data of the footwall  
596 dacite lava at the Ezuri Kuroko deposits: Akito Prefecture: Mining Geology, v. 30, p.  
597 241-250.

598 Sangster, D.F., 1972, Precambrian volcanogenic massive sulfide deposits in Canada: a  
599 review: Geological Survey of Canada paper 72-22, 44 p.

600 Schardt, C., Cooke, D.R., Gemmell, J.B., and Large, R.R., 2001, Geochemical modelling  
601 of the zoned footwall alteration pipe, Hellyer volcanic-hosted massive sulfide  
602 deposit, western Tasmania, Australia: Economic Geology, v. 96, p. 1037-1054.

603 Sharpe, R., 1991, The Hellyer baritic and siliceous caps: Unpublished B.Sc. dissertation,  
604 Honors thesis, Hobart, University of Tasmania, 114 p.

605 Solomon, M., and Zaw, K., 1997, Formation on the sea floor of the Hellyer volcanogenic  
606 massive sulfide deposit: Economic Geology, v. 92(6), p. 686-695.

1  
2  
3  
4  
5  
6  
7  
8  
9  
10  
11  
12  
13  
14  
15  
16  
17  
18  
19  
20  
21  
22  
23  
24  
25  
26  
27  
28  
29  
30  
31  
32  
33  
34  
35  
36  
37  
38  
39  
40  
41  
42  
43  
44  
45  
46  
47  
48  
49  
50  
51  
52  
53  
54  
55  
56  
57  
58  
59  
60  
61  
62  
63  
64  
65

607 Spear, F., 1993, Metamorphic phase equilibria and pressure-temperature-time paths:  
608 Mineralogical Society of America, Washington, D. C., 799 p.

609 Stanley, C.R., and Madeisky, H.E., 1994, Lithogeochemical exploration for hydrothermal  
610 ore deposits using Pearce element ratio analysis: Alteration and alteration processes  
611 associated with ore forming systems, Geological Association of Canada Short  
612 Course Notes, v. 11, p. 193-211.

613 Tessier, A.C., 1990, Structural evolution and host dilatation during emplacement of gold-  
614 bearing quartz veins at Perron deposit, Val-d'Or, Québec: Unpublished M.Sc. thesis,  
615 Kingston, Ontario, Queen's University, 242 p.

616 Tremblay, A., 2001, Postmineralisation fault in the Beaufor gold deposit, Abitibi  
617 Greenstone belt, Canada: geometry, origin and tectonic implications for the Val-D'Or  
618 mining district: Economic Geology, v. 96, p. 509-524.

619 Trépanier, S., 2009, Guide pratique d'utilisation de différentes méthodes de traitement de  
620 l'altération et du métasomatisme./ Review of method for the recognition and  
621 quantification of alteration and metasomatism: Consorem report 2008-07 (report in  
622 French, available at: [http://www.consorem.ca/rapports\\_publics.html](http://www.consorem.ca/rapports_publics.html)).

623 Trépanier, S., 2012, Norme Lithomodeleur./ Lithomodeleur norm: Consorem report  
624 2011-04 (report in French, available at:  
625 [http://www.consorem.ca/rapports\\_publics.html](http://www.consorem.ca/rapports_publics.html)).

626 Waters, J.C., and Wallace, D.B., 1992, Volcanology and sedimentology of the host  
627 succession to the Hellyer and Que River volcanic-hosted massive sulfide deposits,  
628 northwestern Tasmania: Economic Geology, v. 87(3), p. 650-666.

1  
2  
3  
4  
5  
6  
7  
8  
9  
10  
11  
12  
13  
14  
15  
16  
17  
18  
19  
20  
21  
22  
23  
24  
25  
26  
27  
28  
29  
30  
31  
32  
33  
34  
35  
36  
37  
38  
39  
40  
41  
42  
43  
44  
45  
46  
47  
48  
49  
50  
51  
52  
53  
54  
55  
56  
57  
58  
59  
60  
61  
62  
63  
64  
65

630 **Figure captions**

631

632 **Fig. 1** – Exploded view of the main ACFMNK tetrahedron of facies 2SV350.

633 **Fig. 2** – Exploded view of the main ACFMNK tetrahedron of facies 2SV450.

634 **Fig. 3** – Exploded view of the main ACFMNK tetrahedron of facies 2AMP575.

635 **Fig. 4** – Calculation sequence of CONSONORM\_LG (see text for details).

636 **Fig. 5** – Binary diagrams comparing the normative and observed minerals of the Touquoy  
637 (A) and Beaufor (B) deposits. The normative minerals are calculated for the 2SV350  
638 facies.

639 **Fig. 6** – Box plots and binary diagram displaying the alteration indexes calculated for the  
640 Touquoy (A), Heyller (B), Beaufor (C) and Montauban (D) deposits.

641

642

643

644 **Table caption**

645 Table 1: Mineral reactions used to adjust the parageneses for FeO-rich rocks

646 Table 2: Mineral reactions used to solve silica deficits

647 Table 3: WITHOUTCO2 indexes for Na, K, Ca, Fe-Mg and Al alterations

648 Table 4: WITHCO2 indexes for carbonatation-type alteration

649 Table 5: Threshold values of alteration indexes for magmatic rocks

650

651

652

653

1  
2  
3  
4 654 **SUPPORTING INFORMATION**

- 5  
6  
7 655 • **File 1:** copy of the CONSONORM\_LG code, and instructions for importing it  
8  
9 656 into Microsoft Visual Studio software.

10  
11 657  
12  
13  
14 658  
15  
16 659  
17  
18  
19 660 **ANNEX A: CONSONORM\_LG CODE**

20  
21 661 CONSONORM\_LG is provided as three Visual Basic .NET classes, compatible with  
22  
23 662 .NET version 3.5 and later. The first class – CONSONORM\_LG.vb – contains the  
24  
25 663 calculation sequence for a single rock sample. The second class – FormMain.vb – serves  
26  
27 664 as an interface with the user; it is used to input options and data to the code from a .txt  
28  
29 665 file, to calculate the norm and indexes for several samples and to output the data as a .txt  
30  
31 666 file. The third class – TypeDataMx.vb – defines geochemical data types.

32  
33  
34 667 The code contained in these three .NET classes is copied to a .pdf file (see supplementary  
35  
36 668 material). This file contains instructions for integrating the code into the Microsoft Visual  
37  
38  
39 669 Studio software, as well as instructions about input data format.

40  
41  
42  
43 670 The MathNet.Numerics.LinearAlgebra module was also used to define matrices (see  
44  
45 671 <http://numerics.mathdotnet.com>). This .NET compatible module is required to compile  
46  
47 672 the VB code properly.

48  
49  
50  
51 673

52  
53 674

54  
55 675  
56  
57  
58  
59  
60  
61  
62  
63  
64  
65

## ANNEX B: CONSONORM\_LG MINERALS

Mineral	$\sigma$	Formula	Mineral	$\sigma$	Formula
Albite	2.63	NaAlSi <sub>3</sub> O <sub>8</sub>	Pyrope	3.56	Mg <sub>3</sub> Al <sub>2</sub> Si <sub>3</sub> O <sub>12</sub>
Almandine	4.32	Fe <sub>3</sub> Al <sub>2</sub> Si <sub>3</sub> O <sub>12</sub>	Pyrophyllite	2.81	Al <sub>2</sub> Si <sub>4</sub> O <sub>10</sub> (OH) <sub>2</sub>
Andalusite	3.15	Al <sub>2</sub> SiO <sub>5</sub>	Quartz	2.65	SiO <sub>2</sub>
Anorthite	2.75	CaAl <sub>2</sub> Si <sub>2</sub> O <sub>8</sub>	Serpentine	2.54	Mg <sub>6</sub> Si <sub>4</sub> O <sub>10</sub> (OH) <sub>8</sub>
Anthophyllite_FE	3.8	Fe <sub>7</sub> Si <sub>8</sub> O <sub>22</sub> (OH) <sub>2</sub>	Staurolite_FE	3.64	Fe <sub>2</sub> Al <sub>9</sub> Si <sub>4</sub> O <sub>20</sub> (OH) <sub>4</sub>
Anthophyllite_MG	3.67	Mg <sub>7</sub> Si <sub>8</sub> O <sub>22</sub> (OH) <sub>2</sub>	Staurolite_MG	3.54	Mg <sub>2</sub> Al <sub>9</sub> Si <sub>4</sub> O <sub>20</sub> (OH) <sub>4</sub>
Biotite_FE	3.34	KFe <sub>3</sub> AlSi <sub>3</sub> O <sub>10</sub> (OH) <sub>2</sub>	Talc	2.75	Mg <sub>3</sub> Si <sub>4</sub> O <sub>10</sub> (OH) <sub>2</sub>
Biotite_MG	2.83	KMg <sub>3</sub> AlSi <sub>3</sub> O <sub>10</sub> (OH) <sub>2</sub>	Tremolite	3.05	Ca <sub>2</sub> Mg <sub>5</sub> Si <sub>8</sub> O <sub>22</sub> (OH) <sub>2</sub>
Brucite	2.39	MgOOH	Ankerite	3.05	CaFe(CO <sub>3</sub> ) <sub>2</sub>
Chlorite_FE	3.3	Fe <sub>10</sub> Al <sub>4.5</sub> Si <sub>5.5</sub> O <sub>20</sub> (OH) <sub>16</sub>	Calcite	2.71	CaCO <sub>3</sub>
Chlorite_MG	2.75	Mg <sub>10</sub> Al <sub>4.5</sub> Si <sub>5.5</sub> O <sub>20</sub> (OH) <sub>16</sub>	Dolomite	2.84	CaMg(CO <sub>3</sub> ) <sub>2</sub>
Chloritoid_FE	3.7	FeAl <sub>2</sub> SiO <sub>5</sub> (OH) <sub>2</sub>	Magnesite	3	MgCO <sub>3</sub>
Chloritoid_MG	3.57	MgAl <sub>2</sub> SiO <sub>5</sub> (OH) <sub>2</sub>	Rhodochrosite	3.69	MnCO <sub>3</sub>
Cordierite_FE	2.67	Fe <sub>2</sub> Al <sub>4</sub> Si <sub>5</sub> O <sub>18</sub>	Siderite	3.96	FeCO <sub>3</sub>
Cordierite_MG	2.48	Mg <sub>2</sub> Al <sub>4</sub> Si <sub>5</sub> O <sub>18</sub>	Hematite	5.28	Fe <sub>2</sub> O <sub>3</sub>
Diaspore	3.4	AlOOH	Ilmenite	4.79	FeTiO <sub>3</sub>
Diopside	3.26	CaMgSi <sub>2</sub> O <sub>6</sub>	Magnetite	5.15	Fe <sub>3</sub> O <sub>4</sub>
Epidote	3.3	Ca <sub>2</sub> Al <sub>3</sub> Si <sub>3</sub> O <sub>12</sub> (OH)	Rutile	4.8	TiO <sub>2</sub>
Fayalite	4.66	Fe <sub>2</sub> SiO <sub>4</sub>	Titanite	3.48	CaTiSiO <sub>4</sub> (OH)
Ferroactinolite	3.51	Ca <sub>2</sub> Fe <sub>5</sub> Si <sub>8</sub> O <sub>22</sub> (OH) <sub>2</sub>	Arsenopyrite	6.19	FeAsS
Forsterite	3.22	Mg <sub>2</sub> SiO <sub>4</sub>	Chalcopyrite	4.19	CuFeS <sub>2</sub>
Grossular	3.59	Ca <sub>3</sub> Al <sub>2</sub> Si <sub>3</sub> O <sub>12</sub>	Galena	7.4	PbS
Grunerite	3.66	Fe <sub>7</sub> Si <sub>8</sub> O <sub>22</sub> (OH) <sub>2</sub>	Millerite	5.5	NiS
Hedenbergite	3.68	CaFeSi <sub>2</sub> O <sub>6</sub>	Molybdenite	5	MoS
Hornblende_FE	3.38	Ca <sub>2</sub> Fe <sub>5</sub> AlSi <sub>7</sub> O <sub>22</sub> (OH) <sub>2</sub>	Pyrite	5.01	FeS <sub>2</sub>
Hornblende_MG	2.96	Ca <sub>2</sub> Mg <sub>5</sub> AlSi <sub>7</sub> O <sub>22</sub> (OH) <sub>2</sub>	Sphalerite	4.08	ZnS
Leucite	2.48	KAlSi <sub>2</sub> O <sub>6</sub>	Anhydrite	2.35	CaSO <sub>4</sub>
Muscovite	2.83	KAl <sub>3</sub> Si <sub>3</sub> O <sub>10</sub> (OH) <sub>2</sub>	Apatite	3.19	Ca <sub>5</sub> P <sub>3</sub> O <sub>12</sub> (OH)
Nepheline	2.61	NaAlSi <sub>3</sub> O <sub>8</sub>	Chromite	5.09	FeCr <sub>2</sub> O <sub>4</sub>
Orthoclase	2.56	KAlSi <sub>3</sub> O <sub>8</sub>	Halite	2.17	NaCl
Paragonite	2.78	NaAl <sub>3</sub> Si <sub>3</sub> O <sub>10</sub> (OH) <sub>2</sub>	Sylvite	2	KCl



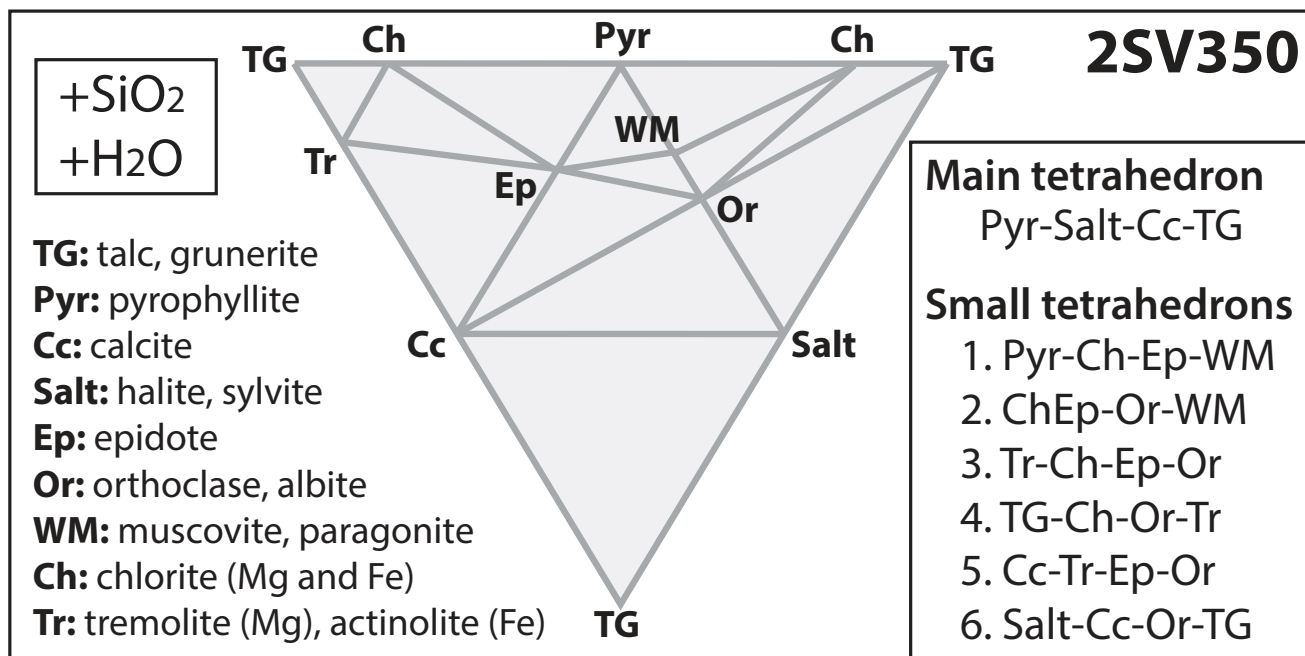


**Fig. 1**

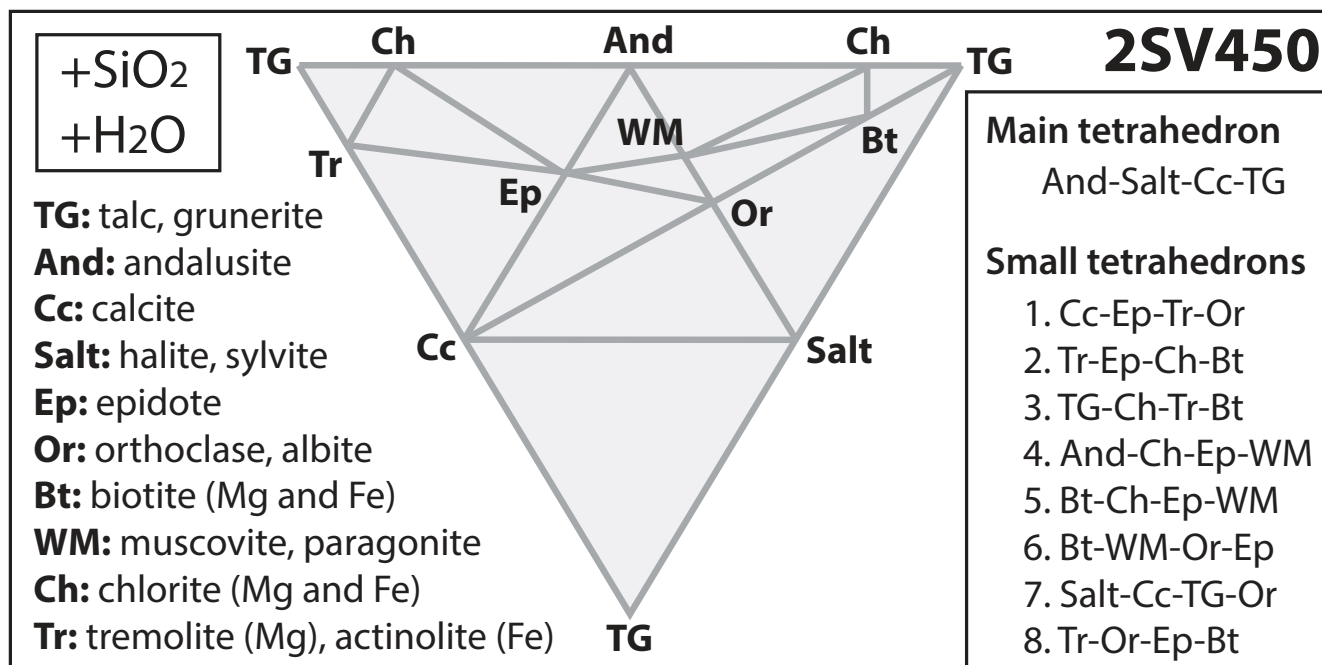


**Fig. 2**

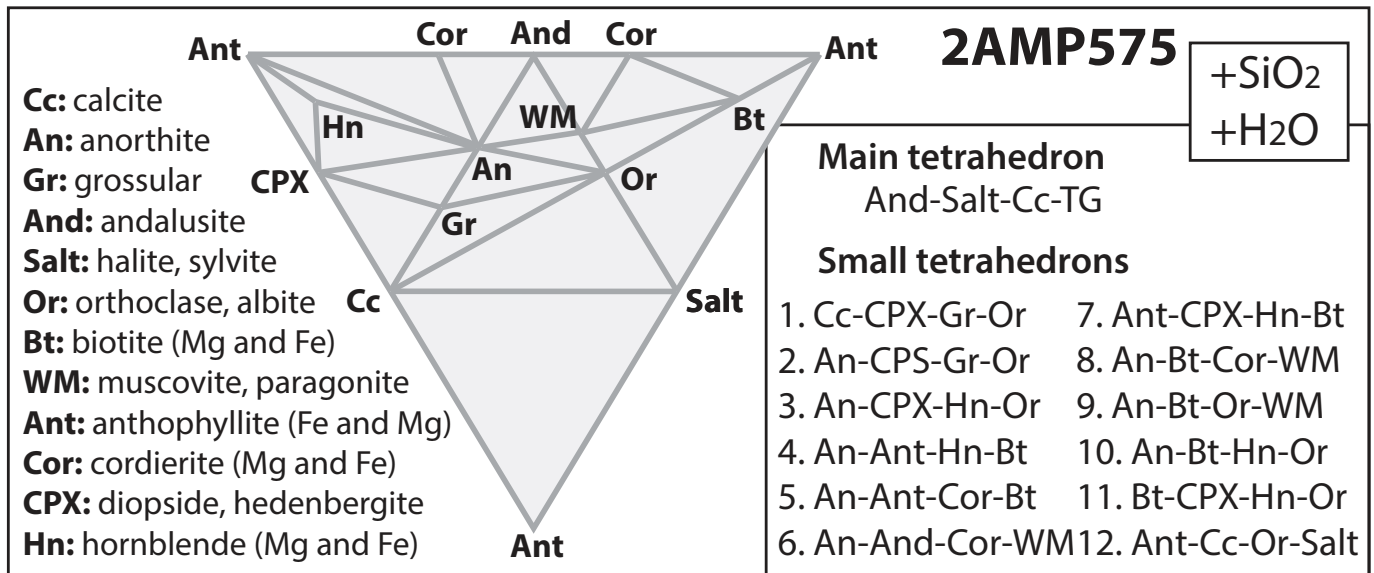


**Fig. 3**

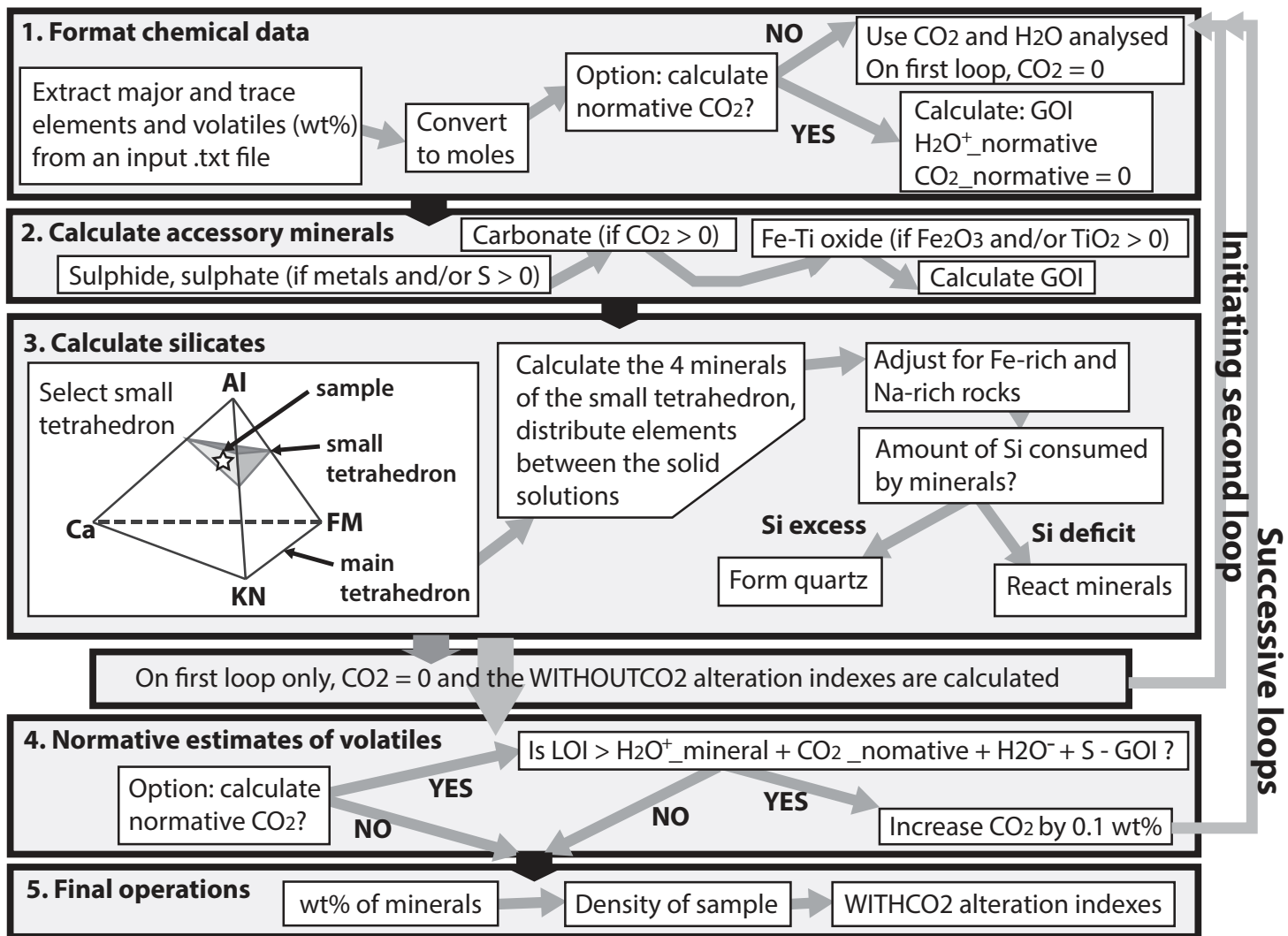


Fig. 4

Figure 5

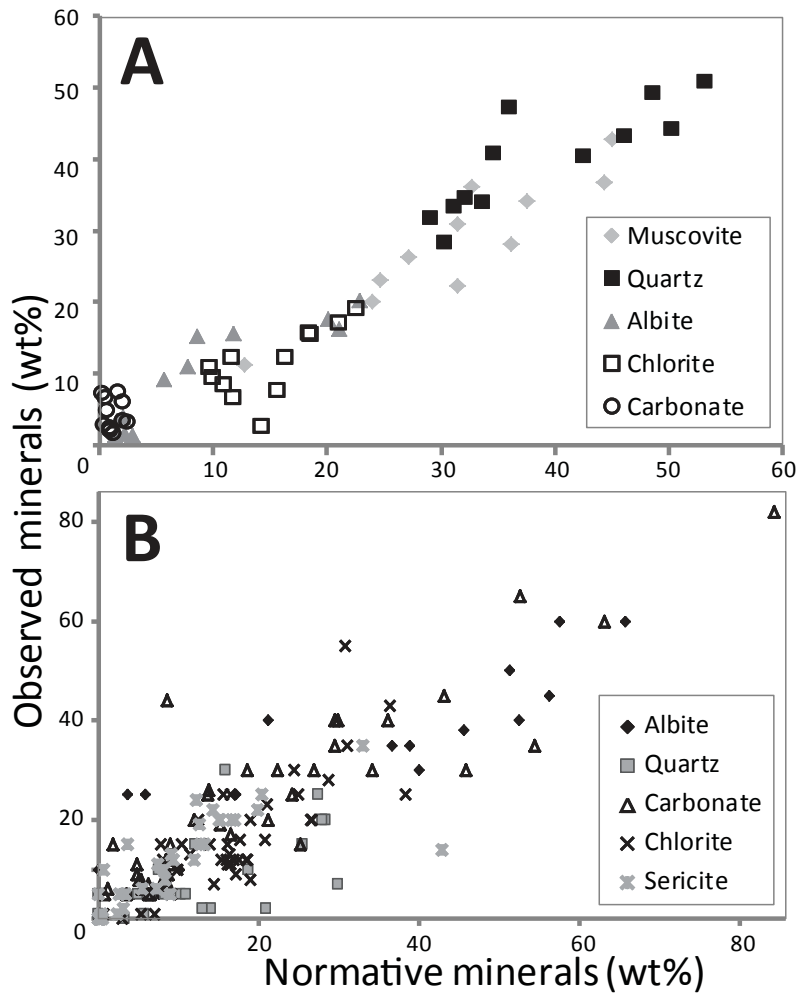
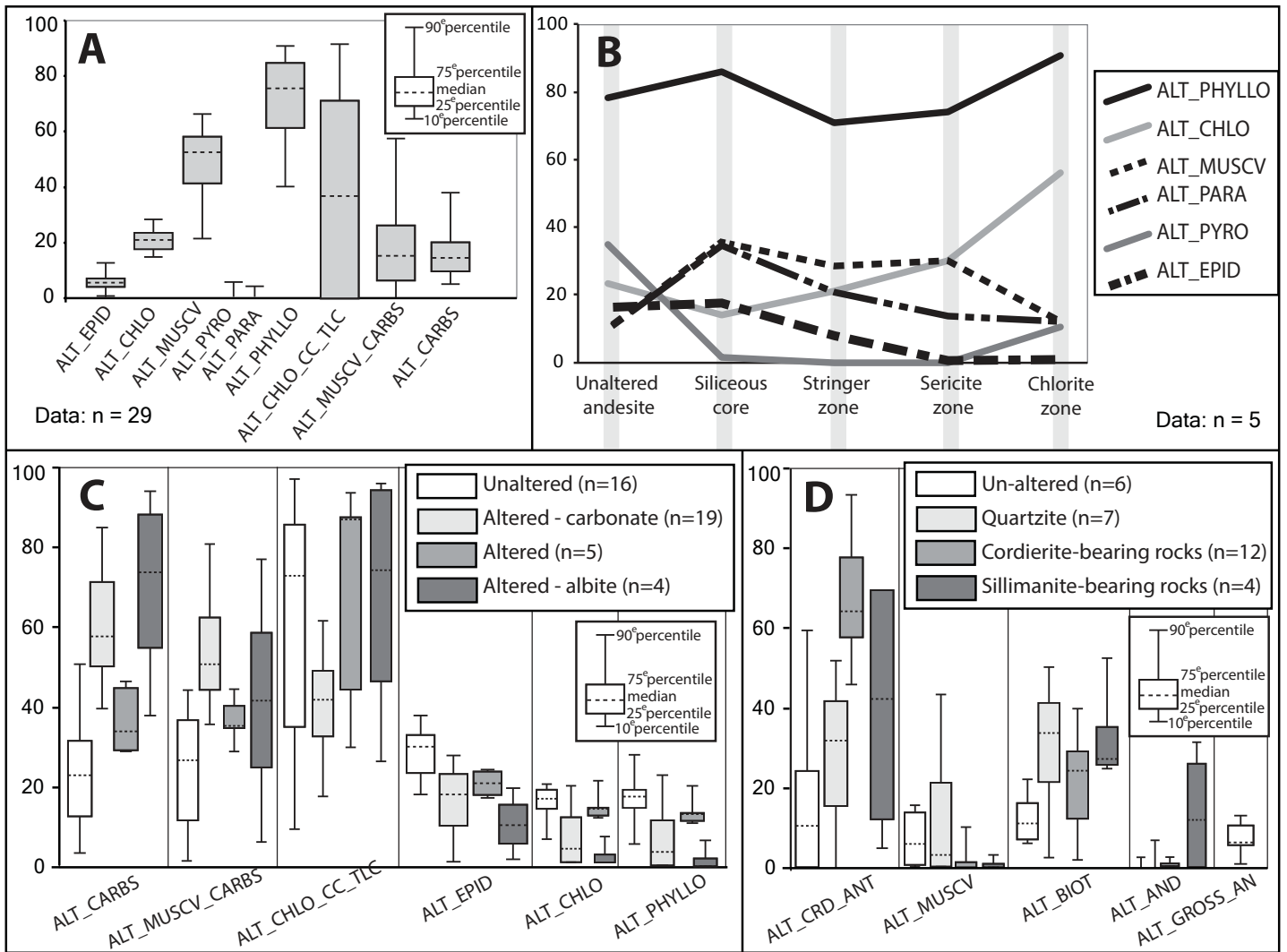


Fig. 5

Figure 6



**Fig. 6**

Table 1: Mineral reactions used to adjust the parageneses for FeO-rich rocks

Facies	Reactions performed	Condition
2SV450	chlorite + 7.75 andalusite + 2.5 H <sub>2</sub> O --> 10 chloritoid + 3.25 quartz 0.516 chlorite + 0.516 muscovite --> 2.161 chloritoid + 2.161 biotite + 0.677 quartz + 1.709 H <sub>2</sub> O	Mg#* <0.3 and muscovite there
2SV450	chlorite + 7.75 andalusite + 2.5 H <sub>2</sub> O --> 10 chloritoid + 3.25 quartz	Mg# <0.65 and epidote there
2AMP575	7.5 cordierite + 5 muscovite --> 5 biotite + 20 andalusite + 17.5 quartz 3.5 cordierite + H <sub>2</sub> O --> anthophyllite + 7 andalusite + 1.25 H <sub>2</sub> O	Mg# <0.55 and muscovite there
2AMP575	9 andalusite + 0.286 anthophyllite + 1.714 H <sub>2</sub> O --> staurolite + 2.785 quartz 15.5 andalusite + 2 biotite + 6 H <sub>2</sub> O --> 3 staurolite + 2 muscovite + 3.5 quartz staurolite + 1.64 anthophyllite --> 4.5 almandine + 3.643 quartz + 3.643 H <sub>2</sub> O 70 staurolite + 3.833 biotite + 9.5 quartz --> 4.5 almandine + 3.833 muscovite + 3.833 H <sub>2</sub> O	Mg# <0.3 and muscovite there
2AMP575	2 cordierite + 5/7 anthophyllite --> 3 almandine + 63/7 quartz + 5/7 H <sub>2</sub> O	Mg# <0.4 and anorthite there

\*Mg# = MgO/(MgO+FeO) molar, calculated with the bulk of FeO and MgO.

Table 2: Mineral reactions used to solve silica deficits

<b>Facies</b>	<b>Reaction</b>
2SV350, 2SV450	2 talc + 2 H <sub>2</sub> O --> serpentine + 4 quartz
2SV350	serpentine --> 6 brucite + 4 quartz + 2 H <sub>2</sub> O
2SV450	serpentine --> 3 forsterite + 1 quartz + 4 H <sub>2</sub> O
2AMP575	anthophyllite--> 3.5 forsterite + 4.5 quartz + H <sub>2</sub> O
2SV450, 2AMP575	forsterite + H <sub>2</sub> O --> 2 brucite + 1 quartz
2SV350, 2SV450	pyrophyllite --> diaspore + 2 quartz
All the facies, only if (Na+K) > Al (molar)	albite --> nepheline + 3 quartz  orthoclase --> leucite + 2 quartz



Table 3: WITHOUTCO2 indexes for Na, K, Ca, Fe-Mg and Al alterations

<b>Facies</b>	<b>Indexes</b>	<b>Formula</b>
2SV350, 2SV450	ALT_CHLO*	$100 * (\text{chlorite\_Mg} * 0.75 + \text{chlorite\_Fe}) / \text{SUM}^{**}$
	ALT_MUSCV	$100 * \text{muscovite} / \text{SUM}$
	ALT_EPID	$100 * \text{epidote} / \text{SUM}$
2SV350	ALT_PYRO	$100 * \text{pyrophyllite} / \text{SUM}$
	ALT_PHYLLO***	$100 * (\text{chlorite\_Mg} * 0.75 + \text{chlorite\_Fe} + \text{muscovite} + \text{paragonite} + \text{pyrophyllite}) / \text{SUM}$
2SV450	ALT_CTD	$100 * (\text{chloritoid\_Mg} + \text{chloritoid\_Fe}) / \text{SUM}$
	ALT_PHYLLO	$100 * (\text{chlorite\_Mg} * 0.75 + \text{chlorite\_Fe} + \text{muscovite} + \text{andalusite} + \text{biotite} + \text{Chloritoid}) / \text{SUM}$
2SV450, 2AMP575	ALT_BIOT	$100 * \text{biotite} / \text{SUM}$
	ALT_AND	$100 * \text{andalusite} / \text{SUM}$
2AMP575	ALT_MUSCV	$100 * \text{muscovite} / \text{SUM}$
	ALT_GROSS_AN	$100 * (\text{grossular} + \text{anorthite} * 0.5) / \text{SUM}$
	ALT_STD_GRT	$100 * (\text{staurolite} + \text{almandine} + \text{pyrope}) / \text{SUM}$
	ALT_CRD_ANTH	$100 * (\text{cordierite} + \text{anthophyllite}) / \text{SUM}$

\*ALT\_CHLO: the 0.75 factor is used to decrease the effect of mafic, naturally chlorite rich protoliths, on the values of this alteration index.

\*\*SUM = sum of all minerals (with chlorite\_Mg multiplied by 0.75) except quartz and sulfides.

\*\*\*ALT\_PHYLLO: index similar to the IFRAIS index of NORMAT (Piché and Jébrak 2004).

Table 4: WITHCO2 indexes for carbonation-type alteration

<b>Facies</b>	<b>Indexes</b>	<b>Formula</b>
2SV350	ALT_CHLO_CC_TLC	100 * (chlorite - chlorite_WITHOUTCO2 + calcite + talc) / SUM*
	ALT_MUSCV_CARBS	100 * (ankerite + dolomite + magnesite + siderite + muscovite - muscovite_WITHOUTCO2) / (SUM + orthoclase + muscovite)
2SV350, 2SV450	ALT_CARBS**	100 * (calcite + dolomite + ankerite + magnesite + siderite) / SUM

\*SUM: sum of all FeO-, MgO- or/and CaO-bearing minerals, except sulfides.

\*\*ALT\_CARBS: similar to the IPAF index of NORMAT (Piché and Jébrak 2004).

Table 5: Threshold values of alteration indexes for magmatic rocks

<b>Facies</b>	<b>Indices</b>	<b>Felsic rocks</b>
2SV350, 2SV450	ALT_CARBS, ALT_CHLO_CC_TLC	> 20 (F); > 0 (I, M, UM*)
	ALT_EPID	> 15 (F); > 30 (I); > 20 (M); > 0 (UM)
	ALT_CHLO, ALT_PHYLLO	> 5-10 (F); > 15 (I, M, UM)
All	ALT_MUSCV, ALT_MUSCV_CARBS	> 5-10 (F); > 0 (I, M, UM)
	ALT_PARA, ALT_PYRO, ALT_CTD, ALT_AND	> 0 (F, I, M, UM)
2AMP575	ALT_GROSS_AN	> 10 (F); > 15 (I); > 10 (M); > 5 (UM)
	ALT_BIOT	> 10 (F, I, M, UM)
	ALT_CRD_ANTH	> 0 (F); > 10 (I, M); > 25 (UM)

\*F, I, M and UM stand for felsic (F), intermediate (I), mafic (M) and ultramafic (UM)

magmatic rocks.